

Target driven visual navigation exploiting object relationships

Yiding Qiu*

Anwesan Pal*

Henrik I. Christensen

Abstract—Recently target driven visual navigation strategies have gained a lot of popularity in the computer vision and reinforcement learning community. Unfortunately, most of the current research tends to incorporate sensory input into a reward based learning approach, with the hope that a robot can implicitly learn its optimal actions through recursive trials. These methods seldom generalize across domains as they fail to exploit natural environment object relationships. We present Memory-utilized Joint hierarchical Object Learning for Navigation in Indoor Rooms (MJOLNIR)¹, a target-driven visual navigation algorithm, which considers the inherent relationship between target objects, along with the more salient parent objects occurring in its surrounding. Extensive experiments conducted across multiple environment settings show $\approx 30\%$ improvement over the existing state-of-the-art navigation methods in terms of the success rate. We also show that our model learns to converge much faster than other algorithms. We will make our code publicly available for use in the scientific community.

I. INTRODUCTION

Prior knowledge is key to making an inference of the physical world. Human beings are able to perform complex tasks such as target-driven navigation efficiently, with implicit memorization of relationships between objects. For example, to find an object such as a “toaster” in the kitchen, the most natural thing to do is to look for a set of plausible objects which are likely to be nearby the toaster. Inherently, these “parent objects” have either a spatial or semantic relationship with the target object, and are likely to be more salient in comparison. This is depicted in Figure 1. Unfortunately, we rarely use these inferences in robot navigation. This is primarily because of two main challenges - (i) to efficiently represent prior knowledge in the form of a hierarchical “parent-target” object relationship, and (ii) to incorporate the learnt prior knowledge effectively into a robot task which can generalize across previously unseen domains.

Most of the existing research [1], [2], [3] in this area tends to aggregate sensory input into a meaningful state, which is then served to a reinforcement learning (RL) system, with the hope that the robot can learn to solve the navigation problem implicitly through trials. Zhu *et al.*[1] proposed to solve this problem by finding the similarity between current image and the image of the target object through a trained Siamese Network [4]. The work of Wortsman *et al.*[3] incorporated a meta-learning framework where the agent learns from

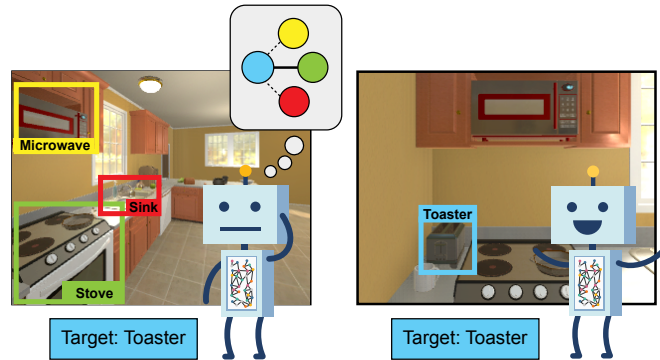


Fig. 1: Illustration of the parent-target relationship. Upon seeing a set of parent objects (left image), the agent learns to associate the correct parent (Stove, here) to the target object (Toaster, here) from the knowledge graph, and tries to search in its neighborhood to successfully locate the target object (right image). [Best when viewed in color]

interactions even during the inference state. However, neither of these methods utilize any prior information or semantic context. Two approaches which are closest to ours are the contributions of Yang *et al.*[2], and Druon *et al.*[5]. In [2], semantic priors in the form of knowledge graphs are used to capture object-object relationships. Yet, the relationship strength between the connected objects in their graph is not utilized. Also, critical information pertaining to an object’s spatial location is missing. Recently, [5] introduced the concept of a *context grid* where they modeled the spatial and language similarity between different objects as a 16×16 grid. However, they do not utilize any prior information into their model, and their action space is also quite different from ours. Moreover, since their code was only recently released, we could not implement their algorithm at the time of writing this paper.

One of the most challenging aspects of reinforcement learning algorithms is the design of a state space which is representative of the agent’s surrounding. A major contribution of this paper lies in the definition of the state space such that the RL model can successfully learn to exploit the object-object relationship. While implementing other algorithms [1], [2], [3], it was observed that even though the convergence during training stage was extremely fast, they gave a relatively poor performance during testing. A possible reason for this is that perhaps the agent is simply learning to memorize the training setting after a certain number of episodes, and thus it fails to generalize to a novel scene. The adaptive gradient of Wortsman *et al.*[3] alleviates

*Equal Contribution

Contextual Robotics Institute, University of California, San Diego.
La Jolla, CA 92093, USA.

{yiqiu, a2pal, hichristensen}@eng.ucsd.edu

¹Supplementary material including code and the videos of the different experiments are available at <https://sites.google.com/eng.ucsd.edu/mjolnir>.

this problem to some extent. Nevertheless, it doesn't remove it completely since it does not consider any prior memory into account. In contrast, our representative state leverages the correct balance of prior context and current observation to provide sufficient information about the surrounding during training, while simultaneously being abstract enough to generalize to a different room layout during testing.

The remainder of the paper is organized as follows. In Section II, we discuss related work, followed by the task definition in Section III. The core ideas behind our approach are described in Section IV. In Section V we discuss the dataset used and the overall experimental design and results, before we summarize the work and outline future challenges in Section VI.

II. RELATED WORK

A. Map vs map-less navigation approaches

Traditional approaches in visual navigation involved formalizing this as an obstacle avoidance problem, where the agent learns to navigate in its environment through a collision-free trajectory. This is done either in the form of offline maps [6], [7], [8], [9], or online maps [10], [11], [12], [13], [14], [15] generated through Simultaneous Localization and Mapping (SLAM) techniques. Given this map as input, the typical approach was to employ a path planning algorithm such as A* [16] or RRT* [17] to generate a collision-free trajectory to the goal. The limitation of these algorithms is that it might not be possible to have a pre-computed map of the environment. Generating a rich semantic map online is also a non-trivial task. With the advent of deep learning, the focus has instead shifted towards methods which are map-less [18], [19], [20], [21], [22], meaning that the representations can be learnt over time through interactions. However, most of these algorithms are not suited for finding specific target objects in a previously unseen environment. In contrast, our approach solves the target-driven navigation problem entirely using only visual inputs without the need of a pre-computed map.

B. PointGoal navigation vs Target-driven navigation

PointGoal navigation [23] refers to the problem where an agent starts from a randomly chosen pose and learns to navigate to a specific target point, usually specified in terms of 2D/3D coordinates relative to the agent. Lately, there has been some research [24], [25] in this area. However, it is still an ill-defined problem in a realistic setting, thereby making comparison difficult [26]. Target-driven navigation refers to the problem where the agent instead learns to navigate to a specified target object while successfully avoiding obstacles. These tasks usually require some prior knowledge about the environment which can be useful for navigation [1], [2], [3], [5]. Our approach falls in this category, but involves learning a robust contextual object-object relationship.

C. Role of learning Semantic Context

Learning semantic context of the surrounding world is an important research topic in the computer vision and

robotics community. However, most of the existing work [27], [28], [29], [30], [31], [32] surrounds static settings such as object detection, semantic segmentation, activity recognition etc. Recently, object-object relationship modeling has been studied for tasks such as image retrieval [33] using scene graphs, visual relation detection [34], visual question-answering [35], [36], place categorization [37], and driver saliency prediction [38]. In this paper, we propose an algorithm which successfully learns to exploit hierarchical object relationships for target-driven visual navigation.

D. Reward Shaping for Policy Networks

Reward shaping is a method in reinforcement learning for engineering a reward function in order to provide more frequent feedback on appropriate behaviors [39]. In general, defining intermediate goals or sub-rewards for an interaction-based learning algorithm is non-trivial, since the environment model is not always known. However, a divide-and-conquer approach is often imperative to exploit the latent structure of a task to enable efficient policy learning [40], [41], [42]. Specifically, for the target-driven visual navigation problem, it is important to learn the inherent "parent-target" object relationship for providing a meaningful feedback to the end-to-end training. For the policy network, we use the Asynchronous Advantage Actor-Critic (A3C) [43] algorithm to sample the action and the value at each step as per the approach of other models [1], [2], [3].

III. TASK DEFINITION

The goal of our visual navigation problem is to find a target object, defined through a set $T = \{t_1, \dots, t_N\}$, in a given room. At each state, the model takes the current observation, prior scene context, and target information as input. Using this, the agent can sample an action a from its trained policy, where $a \in A = \{\text{MoveAhead}, \text{RotateLeft}, \text{RotateRight}, \text{LookUp}, \text{LookDown} \text{ and } \text{Done}\}$. The MoveAhead action takes the agent forward by 0.25 meters, while the RotateLeft and RotateRight actions rotate it by 45 degrees. Finally, the Look action tilts the camera up/down by 30 degrees. An episode is considered a "success", if the target object is visible, meaning the agent can detect it in the current frame, and is within a distance of 1.5 meters from it. If the "Done" action is sampled while this criterion is not met, the episode results in failure.

IV. CONTEXT-BASED VISUAL NAVIGATION

A. Parent-Target Object relationship

In addition to the target objects, we introduce a new set of object classes, defined by the set $P = \{p_1, \dots, p_M\}$. These "parent objects" comprise of the more salient objects present in a room, which also happen to be spatially/semantically related to the target object. For example, "CounterTop" is a parent object in both the "Kitchen" and "Bathroom" scenes, while "Shelf" is a parent object in both "Living room" and "Bedroom". The set of parent objects, P , are manually picked for each room based on the strong correspondences in the input graph (explained in Section IV-B), and the probability

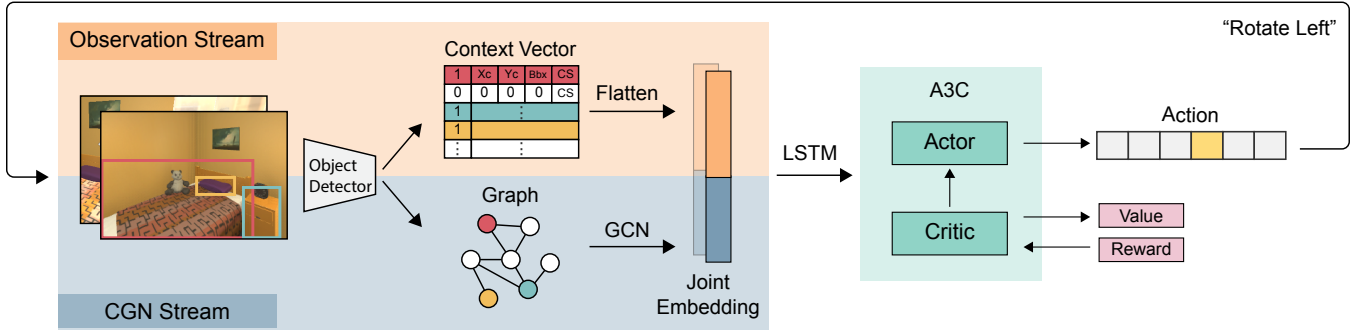


Fig. 2: The entire MJOLNIR architecture. In the Observation stream, we have the GT object detector that gives the context vector for all objects in AI2-THOR. This feature map is combined with the graph embedding from the CGN stream to form a joint embedding. This is then sent to an LSTM cell and finally fed to the A3C model. [Best when viewed in color]

of target-parent relationship $Pr(t \in T | p \in P)$ (explained in IV-D) is calculated based on the spatial closeness of target to each parent using prior knowledge. The aim of the navigation agent is to successfully maneuver to the target object t , while exploiting the relationship that object has with other parent objects present in the room.

B. Construction of Knowledge Graph and the Context vector

One of the early works in target based visual navigation using knowledge graphs was conducted by Yang *et al.*[2]. Our knowledge graph is also constructed using the objects and relationships extracted from the image-captions of the Visual Genome (VG) dataset [44]. However, by pruning a lot of the object (for instance, “armchair” vs “arm chairs”) and relationship (for instance, “near” vs “next to”) aliases, we were able to build a much cleaner graph containing strong relationship correspondences between the VG objects, which also appear in our floorplans.

In addition to the newly constructed graph, we also introduce a novel *context vector*. This 5-D vector gives information regarding the current state of an object o_i , and can be represented as $[b_i, x_c, y_c, b_{box}, CS]^T$. The first element, b_i , is a binary vector specifying whether o_i can be detected in the current frame. The next elements, (x_c, y_c) , and b_{box} correspond to the center (x, y) coordinates of the bounding box of o_i , and its size, both normalized with respect to the image size, respectively. Finally, CS is a number giving the cosine similarity between the respective word embeddings of the object o_i , and the target object $t \in T$. This is expressed as:

$$CS(\mathbf{g}_{o_i}, \mathbf{g}_t) = \frac{\mathbf{g}_{o_i} \cdot \mathbf{g}_t}{\|\mathbf{g}_{o_i}\| \cdot \|\mathbf{g}_t\|}$$

where \mathbf{g} denotes the word embeddings.

C. End-to-end model

In this section, we talk about our entire network, shown in Figure 2. We have two types of input, (i) the Observation Stream, which encodes the the agent’s current observation in the environment, and (ii) the Contextualized Graph Network (CGN) Stream, which embeds the prior memory obtained through a knowledge graph $G = (V, E)$.

For the Observation stream, we tried two variants. Firstly, we use the ResNet-18 [45] conv features to give a holistic representation of the scene. The feature map is then combined with the target object word embedding using point-wise convolution, and flattened to obtain the observation vector. This approach is similar to most state-of-the-art [1], [2], [3] techniques. Secondly, we replaced the ResNet features with the 5-D *context vector* (described in IV-B) for every object in our environment. The resulting *context matrix* $\in \mathbb{R}^{|V| \times 5}$ is then flattened and forms the new observation vector.

The CGN stream contains our knowledge graph, which provides a strong initial guidance to the agent. However, this information, by itself, can be insufficient due to the domain difference between [44] and our environment - AI2-THOR [46]. For this reason, we use the Graph Convolution Networks (GCN) [47] to learn the node embeddings. The structure of our proposed CGN is shown in Figure 3. Given the input graph G , we design the node feature vector X to contain the word embedding of each object. To further include the state information, we concatenated each word embedding with the output of the object detector on the current frame, specified by the $|V| = 101$ -dimensional vector having 1 for the current frame objects, and 0 for others. This is different from the 1000-dimensional class probability used by Yang *et al.*[2]. The reason for this change is two-fold - (i) the probability vector obtained from ResNet-18 [45] is pretrained on the 1000 classes of ImageNet [48], which are quite different from the object list present in our environment - AI2-THOR [46], and (ii) since the pretrained network primarily learns to classify a single object, in the multi-object setting, it is more likely to generate noisy labels. The combined input node features are passed through 2 layers of GCN, to generate a 5-D intermediate embedding. This new feature is then concatenated with the *context vector*, and then fed to another layer of GCN to generate the final graph embedding. The concatenation of the observation vector and the graph embedding results in the joint embedding, which is the input for the A3C model.

To separately highlight the contribution of the changes made to each of the streams, we present two variants of our algorithm. MJOLNIR-r uses ResNet and Glove in the

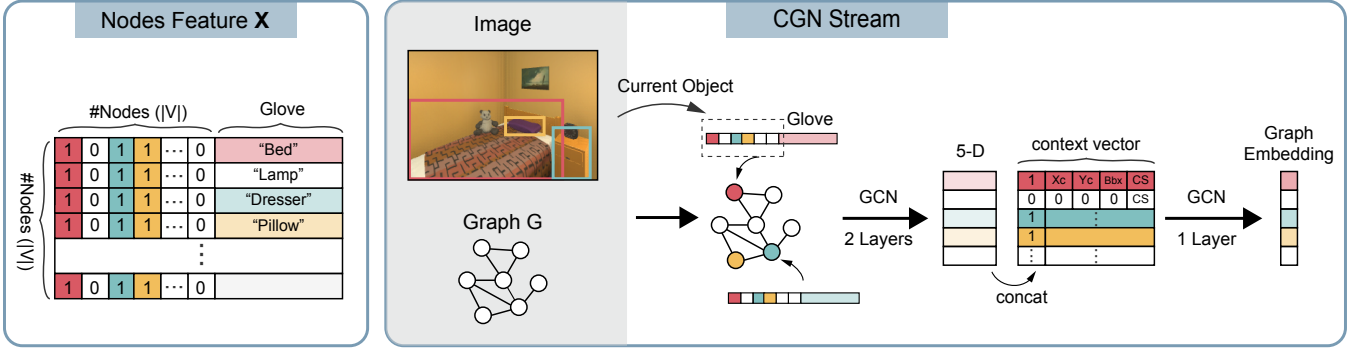


Fig. 3: The novel CGN architecture. The input node feature constitutes the current detected object list and the node object’s glove embedding. This is passed through two layers of GCN. This intermediate embedding is concatenated with the context vector and another layer of GCN is trained on it. [Best when viewed in color]

current observation stream, while only modifying the graph stream from [2] to CGN. MJOLNIR-o uses only the object state context vector as the current observation, along with our CGN stream.

D. Reward

We tune our reward function to correctly learn to exploit the parent-target relationship for the navigation task. The agent in our model receives a “partial reward”, R_p , when a parent object $p \in P$ is visible. This is given by $R_p = R_t * Pr(t|p) * k$, where R_t is the target reward and $k \in (0,1)$ is the scaling factor. We choose $R_t = 5$ and $k = 0.1$ for our experiments. $Pr(t|p)$ is taken from the partial reward matrix M , where each row has the probability distribution of the relative closeness of all the parent objects, to a given target object. The closeness is calculated based on the relative spatial distance between objects present in the floorplans of AI2-THOR. If multiple parent objects are visible, we only choose the one with the maximum R_p . Moreover, the agent does not get this reward the next time it sees the same parent object. This encourages it to explore different parent objects in the room until the target is located. If the “Done” action is sampled, *i.e.* the termination criterion, and t is visible, the agent gets the sum of the goal reward and R_p . In this way, it learns to associate parent objects with a target, as well as the current state. Since the entire network is trained end-to-end, this shaped reward propagates back to the GCN layers, and tunes them to correctly exploit the “parent-target” relationship from the knowledge graph. Finally, if neither the parent nor the target object is visible, the agent gets a negative step penalty of 0.01. The reward for the state s , and action a , is therefore given by:

$$R(s,a) = \begin{cases} R_p, & \text{if } p \text{ is visible} \\ R_t, & \text{if } t \text{ is visible at termination} \\ R_t + R_p, & \text{if both are visible at termination} \\ -0.01, & \text{otherwise} \end{cases}$$

Algorithm 1 summarizes the above explained process.

Algorithm 1: Reward Shaping for MJOLNIR

Input: state s , action a , target $t \in T$, SeenList

Data: target reward R_t , parent reward table M

Function Judge(s, a, t):

```

if  $a \neq$  “DONE” then
  | reward = Partial( $s, t$ )
else if  $a ==$  “DONE” and  $t$  is visible then
  | SeenList = [];
  | reward =  $R_t +$  Partial( $s, t$ );

```

return reward;

Function Partial(s, t):

```

foreach parent  $p_i \in P$  do
  | if  $p_i$  is visible and  $p_i \notin$  SeenList then
  | |  $p \leftarrow \operatorname{argmax} M[t]$ ;
  | | SeenList  $\leftarrow p$ ;
  | |  $R_p = M[t][p] * R_t * k$ 
end

```

return R_p ;

V. EXPERIMENTS AND RESULTS

A. Dataset and Object Description

We use the AI2-THOR (The House Of inteRactions) [46] environment as our platform for the navigation tasks. It consists of 120 photo-realistic floorplans categorized into 4 different room layouts - *Kitchen*, *Living room*, *Bedroom*, and *Bathroom*, thus making 30 plans for each layout. In our experiments, we consider the first 20 rooms from each scene type for the training set, and the remaining 10 rooms for evaluation.

The target object list comprises of the following: *Kitchen* - Toaster, Spatula, Bread, Mug, CoffeeMachine, Apple; *Living room* - Painting, Laptop, Television, RemoteControl, Vase, ArmChair; *Bedroom* - Blinds, DeskLamp, Pillow, AlarmClock, CD; *Bathroom* - Mirror, ToiletPaper, SoapBar, Towel, SprayBottle.

The parent objects were not specified with room layout as they are likely to be large objects which might be present in more than one scene type. This list comprises of: StoveBurner, CounterTop, Sink, Microwave,

TableTop, Fridge, Shelf, Drawer, FloorLamp, Sofa, Bed, NightStand, Desk, Dresser, Cabinet, Toilet, Bathtub, ShowerDoor.

B. Metrics

For fair comparison with other state-of-the-art algorithms, we use the evaluation metrics proposed by [23], and adopted by other target-driven visual navigation algorithms [1], [2], [3], [5]. The Success Rate (SR) is defined as $\frac{1}{N} \sum_{i=1}^N S_i$, while the Success weighted by Path Length (SPL) is given by $\frac{1}{N} \sum_{i=1}^N S_i \frac{l_i}{\max(l_i, e_i)}$. Here, N is the number of episodes, S_i is a binary vector indicating the success of the i -th episode. e_i denotes the path length of an agent episode, and l_i is the optimal trajectory length to any instance of the target object in a given scene from the initial state. We evaluate the performance of all the models on the trajectories where the optimal path length is at least 1 ($L \geq 1$), and at least 5 ($L \geq 5$).

C. Comparison Models

Random - In this model, as each step, the agent randomly samples its actions from the action space with a uniform distribution. **Baseline** - This model closely resembles that of Zhu *et al.*[1], as it comprises of the current observation (in the form of the ResNet-18 features of the current RGB frame) and the target information (in the form of glove embedding of the target object) in its state. **Scene Prior (SP)** - In this model, we preserve the graph network structure of Yang *et al.*[2]. However, instead of concatenating the flattened ResNet-18 and target glove embedding, we perform a point-wise convolution between their respective feature maps, before feeding it to A3C. **SAVN** - In this model [3], the agent keeps learning about its environment through an interactive loss function even during inference time.

D. Implementation details

We built our models based on the publicly available code of [3], using the PyTorch framework. For the word

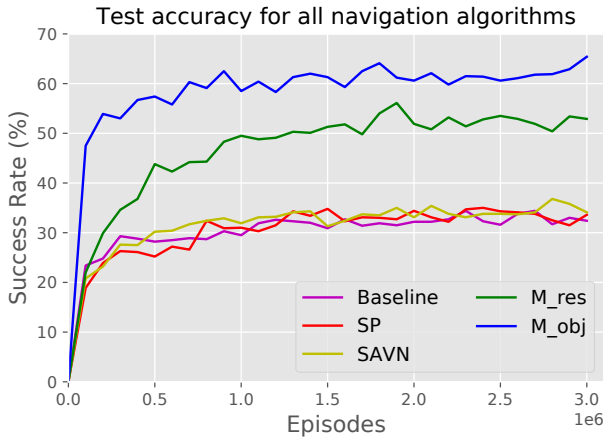
embeddings, we used the 300-D GloVe vectors pretrained on 840 billion tokens of Common Crawl [49]. The A3C model is based on [50], and the model hyperparameters used were: learning rate - 1×10^{-4} , discount factor - 0.99, optimizer - SharedAdam. We used 8 workers for all the models except for SAVN [3], where we could only use 6 workers due to our computational inability to accommodate its large model size. In MJOLNIR-r, the pretrained ResNet-18 model was used to generate the image features, while the simulator’s ground-truth object detector was used to retrieve the information for the context vector used in both MJOLNIR-r and MJOLNIR-o. The agent was trained for 3 million episodes on the offline data from AI2-THOR v1.0.1 [46]. During evaluation, we used 250 episodes for each of the 4 room types, resulting in $250 \times 4 = 1000$ episodes in total. In each episode, the floorplan, target, and the initial agent position was randomly chosen from the evaluation set defined in Section V-A.

E. Results

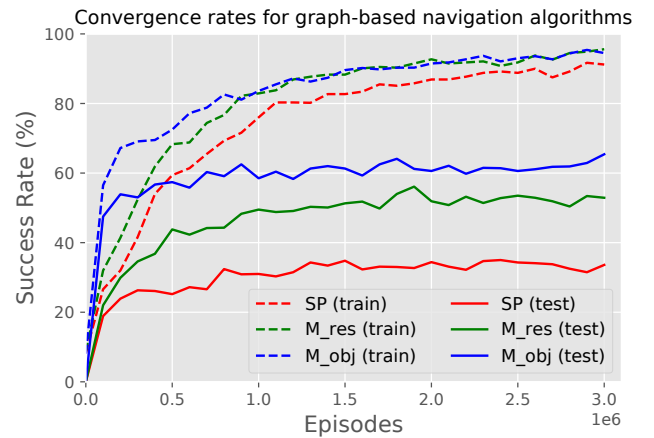
Model	$L \geq 1$		$L \geq 5$	
	SR(%)	SPL(%)	SR(%)	SPL(%)
Random	11.2	5.1	1.1	0.50
Baseline [1]	35.0	10.3	25.0	10.5
Scene-prior [2]	35.4	10.9	23.8	10.7
SAVN [3]	35.7	9.3	23.9	9.4
MJOLNIR-r (our)	54.8	19.2	41.7	18.9
MJOLNIR-o (our)	65.3	21.1	50.0	20.9

TABLE I: Comparison with state-of-the-art visual navigation algorithms

Table I and Figure 4a shows the performance of each of the tested models in terms of Success Rate (SR) and SPL. It can be seen that both of our models significantly outperform the current state-of-the-art. MJOLNIR-o has $\approx 30\%$ increase in SR. This supports our hypothesis that incorporating *context vector* into the state is indeed a better idea than directly using



(a) Test accuracy for all algorithms



(b) Training and test convergence rate for all algorithms

Fig. 4: Test accuracy and convergence rates for all the algorithms

Models	Bathroom		Bedroom		Kitchen		Living Room		Average	
	SR(%)	SPL(%)	SR(%)	SPL(%)	SR(%)	SPL(%)	SR(%)	SPL(%)	SR(%)	SPL(%)
Baseline [1]	53.2	13.4	28.8	9.0	32.4	10.9	35.2	10.0	37.4	10.8
Scene Prior [2]	41.6	13.3	33.6	10.4	26.4	9.1	36.0	9.9	34.4	10.7
SAVN [3]	47.6	14.6	21.6	6.7	34.8	8.3	40.0	9.0	36.9	9.7
MJOLNIR-r (our)	72.8	24.3	41.2	16.9	56.4	21.2	50.8	15.9	55.3	19.6
MJOLNIR-o (our)	82.4	25.1	43.2	14.4	74.8	22.9	50.0	17.9	62.6	20.1

TABLE II: Evaluation results on a per-room basis

ResNet and GloVe features. This is because the semantic information extracted from the scene in this manner is more object-centric, thereby making the target-driven navigation problem easier. It is also important to note here, that the GCN network of [2], which does not include the *context vector* as its node feature, performs poorer than even the baseline [1] and SAVN [3].

Using ResNet in the observation stream, however, is not such a bad idea, as can be seen by the performance of MJOLNIR-r. This is because the ResNet conv features can still capture some contextual information from the current input image. Moreover, using reward shaping to tune the CGN parameters ensures that not only is the prior memory preserved, but the current information containing the parent-target object hierarchy is also appended to it.

In Figure 4b, we analyze the convergence rate of our MJOLNIR with Yang *et al.*[2]. It can be seen that the training and testing SR of our algorithms soars within the first 5 million episodes itself, before saturating. This shows that our models learn to correctly locate targets much faster than others. In contrast, for [2], even though the training SR is quite high ($\approx 90\%$), there is huge drop during the testing performance ($\approx 30\%$), signifying severe overfitting. Finally, Table II gives the comparison of room-wise results.

DONE action	Model	$L \geq 1$		$L \geq 5$	
		SR(%)	SPL(%)	SR(%)	SPL(%)
only sampled	MJOLNIR-r	54.8	19.2	41.7	18.9
	MJOLNIR-o	65.3	21.1	50.0	20.9
	MJOLNIR-o (no_g)	59.0	16.6	41.0	16.9
	MJOLNIR-o (w)	64.7	21.6	46.4	20.6
sampled + env	SAVN	54.4	35.55	37.87	23.47
	MJOLNIR-o	83.1	53.9	71.6	36.9

TABLE III: Ablation study for MJOLNIR

F. Ablation study

We show a number of ablations on MJOLNIR in Table III. MJOLNIR-o (no_g) differs from MJOLNIR-o in that it does not contain the 3rd GCN layer, where we concatenated output of the previous two layers and the *context vector*. Instead, here, we directly feed the previous two-layer output to the joint embedding. In MJOLNIR-o (w), we used a weighted adjacency matrix for the GCN layers. This does not affect the performance significantly as we believe that the object-object relationship is inherently learnt by MJOLNIR-o.

We also evaluated our model with a different stopping criteria. In this case, the agent does not rely only on its sampled “DONE” action to learn the termination action. Instead, it stops even when the environment gives the signal that the target object has been found. We compare our model with the SAVN [3] model using this stopping criteria. The results show that we perform significantly better.

VI. CONCLUSION

In this paper, we introduced MJOLNIR, a novel target-driven visual navigation algorithm that utilizes prior knowledge, and also learns to associate object “closeness” in the form of parent-target hierarchy during training. This is done through the proposed *context vector* which can be easily derived from the output of an object detector. We show that besides the modified input state, knowledge graph, and reward shaping too play a significant role in guiding the agent to search for the target. Extensive experiments conducted show that the agent can successfully find small target objects using the more salient parent object as an anchor. Our model has the ability to generalize across different unseen scenes, and outperforms all other state-of-the-art models.

ACKNOWLEDGEMENT

The authors would like to thank Army Research Laboratory (ARL) W911NF-10-2-0016 Distributed and Collaborative Intelligent Systems and Technology (DCIST) Collaborative Technology Alliance for supporting this research.

REFERENCES

- [1] Y. Zhu, R. Mottaghi, E. Kolve, J. J. Lim, A. Gupta, L. Fei-Fei, and A. Farhadi, “Target-driven visual navigation in indoor scenes using deep reinforcement learning,” in *2017 IEEE international conference on robotics and automation (ICRA)*. IEEE, 2017, pp. 3357–3364.
- [2] W. Yang, X. Wang, A. Farhadi, A. Gupta, and R. Mottaghi, “Visual semantic navigation using scene priors,” *arXiv preprint arXiv:1810.06543*, 2018.
- [3] M. Wortsman, K. Ehsani, M. Rastegari, A. Farhadi, and R. Mottaghi, “Learning to learn how to learn: Self-adaptive visual navigation using meta-learning,” in *The IEEE Conference on Computer Vision and Pattern Recognition (CVPR)*, June 2019.
- [4] G. Koch, “Siamese neural networks for one-shot image recognition,” in *International conference on machine learning*, 2015.
- [5] R. Druon, Y. Yoshidasu, A. Kanazaki, and A. Watt, “Visual object search by learning spatial context,” *IEEE Robotics and Automation Letters*, vol. 5, no. 2, pp. 1279–1286, April 2020.
- [6] O. Khatib, “Real-time obstacle avoidance for manipulators and mobile robots,” in *Autonomous robot vehicles*. Springer, 1986, pp. 396–404.
- [7] J. Borenstein and Y. Koren, “Real-time obstacle avoidance for fast mobile robots in cluttered environments,” in *Proceedings., IEEE International Conference on Robotics and Automation*. IEEE, 1990, pp. 572–577.

- [8] J. Borenstein, Y. Koren *et al.*, "The vector field histogram-fast obstacle avoidance for mobile robots," *IEEE transactions on robotics and automation*, vol. 7, no. 3, pp. 278–288, 1991.
- [9] D. Kim and R. Nevatia, "Symbolic navigation with a generic map," *Autonomous Robots*, vol. 6, no. 1, pp. 69–88, 1999.
- [10] A. DAVISON, "Real-time simultaneous localization and mapping with a single camera," in *Proc. IEEE Intl. Conf. on Computer Vision*, 2003, 2003, pp. 1403–1410.
- [11] J. Engel, T. Schöps, and D. Cremers, "LSD-SLAM: Large-scale direct monocular SLAM," in *European conference on computer vision*. Springer, 2014, pp. 834–849.
- [12] R. Mur-Artal, J. M. M. Montiel, and J. D. Tardos, "ORB-SLAM: a versatile and accurate monocular SLAM system," *IEEE transactions on robotics*, vol. 31, no. 5, pp. 1147–1163, 2015.
- [13] R. Sim and J. J. Little, "Autonomous vision-based exploration and mapping using hybrid maps and rao-blackwellised particle filters," in *2006 IEEE/RSJ International Conference on Intelligent Robots and Systems*. IEEE, 2006, pp. 2082–2089.
- [14] M. Tomono, "3-d object map building using dense object models with sift-based recognition features," in *2006 IEEE/RSJ International Conference on Intelligent Robots and Systems*, Oct 2006, pp. 1885–1890.
- [15] D. Wooden, "A guide to vision-based map building," *IEEE Robotics & Automation Magazine*, vol. 13, no. 2, pp. 94–98, 2006.
- [16] P. E. Hart, N. J. Nilsson, and B. Raphael, "A formal basis for the heuristic determination of minimum cost paths," *IEEE transactions on Systems Science and Cybernetics*, vol. 4, no. 2, pp. 100–107, 1968.
- [17] S. Karaman and E. Frazzoli, "Sampling-based algorithms for optimal motion planning," *The international journal of robotics research*, vol. 30, no. 7, pp. 846–894, 2011.
- [18] C. Chen, A. Seff, A. Kornhauser, and J. Xiao, "Deepdriving: Learning affordance for direct perception in autonomous driving," in *Proceedings of the IEEE International Conference on Computer Vision*, 2015, pp. 2722–2730.
- [19] S. Gupta, J. Davidson, S. Levine, R. Sukthankar, and J. Malik, "Cognitive mapping and planning for visual navigation," in *Proceedings of the IEEE Conference on Computer Vision and Pattern Recognition*, 2017, pp. 2616–2625.
- [20] A. Giusti, J. Guzzi, D. C. Cireşan, F.-L. He, J. P. Rodríguez, F. Fontana, M. Faessler, C. Forster, J. Schmidhuber, G. Di Caro *et al.*, "A machine learning approach to visual perception of forest trails for mobile robots," *IEEE Robotics and Automation Letters*, vol. 1, no. 2, pp. 661–667, 2015.
- [21] C. Linegar, W. Churchill, and P. Newman, "Made to measure: Bespoke landmarks for 24-hour, all-weather localisation with a camera," in *2016 IEEE International Conference on Robotics and Automation (ICRA)*. IEEE, 2016, pp. 787–794.
- [22] P. Saeedi, P. D. Lawrence, and D. G. Lowe, "Vision-based 3-D trajectory tracking for unknown environments," *IEEE transactions on robotics*, vol. 22, no. 1, pp. 119–136, 2006.
- [23] P. Anderson, A. Chang, D. S. Chaplot, A. Dosovitskiy, S. Gupta, V. Koltun, J. Kosecka, J. Malik, R. Mottaghi, M. Savva *et al.*, "On evaluation of embodied navigation agents," *arXiv preprint arXiv:1807.06757*, 2018.
- [24] D. Mishkin, A. Dosovitskiy, and V. Koltun, "Benchmarking classic and learned navigation in complex 3d environments," *arXiv preprint arXiv:1901.10915*, 2019.
- [25] N. Kojima and J. Deng, "To learn or not to learn: Analyzing the role of learning for navigation in virtual environments," *arXiv preprint arXiv:1907.11770*, 2019.
- [26] M. Savva, A. Kadian, O. Maksymets, Y. Zhao, E. Wijmans, B. Jain, J. Straub, J. Liu, V. Koltun, J. Malik *et al.*, "Habitat: A platform for embodied ai research," in *Proceedings of the IEEE International Conference on Computer Vision*, 2019, pp. 9339–9347.
- [27] A. Torralba, K. Murphy, W. Freeman, and M. Rubin, "Context-based vision system for place and object recognition," in *Proceedings Ninth IEEE International Conference on Computer Vision*, 2003.
- [28] D. Hoiem, A. A. Efros, and M. Hebert, "Geometric context from a single image," in *Tenth IEEE International Conference on Computer Vision (ICCV'05) Volume 1*, vol. 1. IEEE, 2005, pp. 654–661.
- [29] A. Rabinovich, A. Vedaldi, C. Galleguillos, E. Wiewiora, and S. Belongie, "Objects in context," in *2007 IEEE 11th International Conference on Computer Vision*. IEEE, 2007, pp. 1–8.
- [30] R. Mottaghi, X. Chen, X. Liu, N.-G. Cho, S.-W. Lee, S. Fidler, R. Urtasun, and A. Yuille, "The role of context for object detection and semantic segmentation in the wild," in *Proceedings of the IEEE Conference on Computer Vision and Pattern Recognition*, 2014, pp. 891–898.
- [31] A. Shrivastava and A. Gupta, "Contextual priming and feedback for faster r-cnn," in *European Conference on Computer Vision*. Springer, 2016, pp. 330–348.
- [32] M. Marszalek, I. Laptev, and C. Schmid, "Actions in context," in *2009 IEEE Conference on Computer Vision and Pattern Recognition*. IEEE, 2009, pp. 2929–2936.
- [33] J. Johnson, R. Krishna, M. Stark, L.-J. Li, D. Shamma, M. Bernstein, and L. Fei-Fei, "Image retrieval using scene graphs," in *Proceedings of the IEEE conference on computer vision and pattern recognition*, 2015, pp. 3668–3678.
- [34] H. Zhang, Z. Kyaw, S.-F. Chang, and T.-S. Chua, "Visual translation embedding network for visual relation detection," in *Proceedings of the IEEE conference on computer vision and pattern recognition*, 2017, pp. 5532–5540.
- [35] J. Johnson, B. Hariharan, L. van der Maaten, L. Fei-Fei, C. Lawrence Zitnick, and R. Girshick, "Clevr: A diagnostic dataset for compositional language and elementary visual reasoning," in *Proceedings of the IEEE Conference on Computer Vision and Pattern Recognition*, 2017, pp. 2901–2910.
- [36] K. Marino, M. Rastegari, A. Farhadi, and R. Mottaghi, "OK-VQA: A visual question answering benchmark requiring external knowledge," in *Proceedings of the IEEE Conference on Computer Vision and Pattern Recognition*, 2019, pp. 3195–3204.
- [37] A. Pal, C. Nieto-Granda, and H. I. Christensen, "DEDUCE: Diverse scene detection methods in unseen challenging environments," in *2019 IEEE/RSJ International Conference on Intelligent Robots and Systems (IROS)*, Nov 2019, pp. 4198–4204.
- [38] A. Pal, S. Mondal, and H. I. Christensen, "Looking at the right stuff - Guided semantic-gaze for autonomous driving," *arXiv preprint arXiv:1911.10455*, 2019.
- [39] E. Wiewiora, *Reward Shaping*. Boston, MA: Springer US, 2010, pp. 863–865.
- [40] D. Tang, X. Li, J. Gao, C. Wang, L. Li, and T. Jebara, "Subgoal discovery for hierarchical dialogue policy learning," in *Proceedings of the 2018 Conference on Empirical Methods in Natural Language Processing*. Brussels, Belgium: Association for Computational Linguistics, Oct.-Nov. 2018, pp. 2298–2309. [Online]. Available: <https://www.aclweb.org/anthology/D18-1253>
- [41] B. Bakker, J. Schmidhuber *et al.*, "Hierarchical reinforcement learning based on subgoal discovery and subpolicy specialization," in *Proc. of the 8-th Conf. on Intelligent Autonomous Systems*, 2004, pp. 438–445.
- [42] S. Goel and M. Huber, "Subgoal discovery for hierarchical reinforcement learning using learned policies," in *AAAI Conference on Artificial Intelligence*, 2003.
- [43] V. Mnih, A. P. Badia, M. Mirza, A. Graves, T. Lillicrap, T. Harley, D. Silver, and K. Kavukcuoglu, "Asynchronous methods for deep reinforcement learning," in *International conference on machine learning*, 2016, pp. 1928–1937.
- [44] R. Krishna, Y. Zhu, O. Groth, J. Johnson, K. Hata, J. Kravitz, S. Chen, Y. Kalantidis, L.-J. Li, D. A. Shamma *et al.*, "Visual genome: Connecting language and vision using crowdsourced dense image annotations," *International Journal of Computer Vision*, vol. 123, no. 1, pp. 32–73, 2017.
- [45] K. He, X. Zhang, S. Ren, and J. Sun, "Deep residual learning for image recognition," in *The IEEE Conference on Computer Vision and Pattern Recognition (CVPR)*, June 2016.
- [46] E. Kolve, R. Mottaghi, W. Han, E. VanderBilt, L. Weihs, A. Her-rasti, D. Gordon, Y. Zhu, A. Gupta, and A. Farhadi, "AI2-THOR: An interactive 3D environment for visual AI," *arXiv preprint arXiv:1712.05474*, 2017.
- [47] T. N. Kipf and M. Welling, "Semi-supervised classification with graph convolutional networks," *arXiv preprint arXiv:1609.02907*, 2016.
- [48] J. Deng, W. Dong, R. Socher, L.-J. Li, K. Li, and L. Fei-Fei, "Imagenet: A large-scale hierarchical image database," in *2009 IEEE conference on computer vision and pattern recognition*. Ieee, 2009, pp. 248–255.
- [49] J. Pennington, R. Socher, and C. D. Manning, "Glove: Global vectors for word representation," in *Proceedings of the 2014 conference on empirical methods in natural language processing (EMNLP)*, 2014, pp. 1532–1543.
- [50] I. Kostrikov, "Pytorch implementations of asynchronous advantage actor critic," <https://github.com/ikostrikov/pytorch-a3c>, 2018.